Imaging Science in Dentistry 2026
https://doi.org/10.5624/isd.20250232

Side- and patient-based performance of a deep learning system based on the results of individual detection of carotid artery calcifications on panoramic radiographs

Yuta Mitsuya[1,†], Chiaki Kuwada[1,†,*], Sujin Yang[2], Yoshitaka Kise[1], Mizuho Mori[1], Yukiko Takashi[1], Masako Nishiyama[1], Natsuho Ishikawa[1], Munetaka Naitoh[1], Eiichiro Ariji[1]

[1]*Department of Oral and Maxillofacial Radiology, Aichi Gakuin University School of Dentistry, Nagoya, Japan*
[2]*Department of Advanced General Dentistry, College of Dentistry, Yonsei University, Seoul, Korea*

ABSTRACT

Purpose: The present study aimed to develop 2 deep learning (DL) systems incorporating detection functions for the diagnosis of carotid artery calcifications (CACs) on panoramic radiographs and to compare their diagnostic performances using CAC-based, side-based, and patient-based evaluations.

Materials and Methods: Panoramic radiographs from 290 patients with CACs and 290 control patients without CACs were used to develop 2 detection models: one designed to detect individual CACs across the entire radiograph (System 1) and another designed to detect CACs within the limited bilateral cervical areas (System 2). CAC-based performance was evaluated using recall, precision, and F1-score. Side-based and patient-based performances were assessed using sensitivity, specificity, positive predictive value, negative predictive value, accuracy, and the area under the receiver operating characteristic curve (AUC).

Results: For System 1, CAC-based recall, precision, and F1-score were 0.81, 0.68, and 0.74, respectively. For System 2, the corresponding values were 0.90, 0.67, and 0.77. Side-based sensitivity, specificity, and AUC were 0.87, 0.80, and 0.83 for System 1, and 0.93, 0.84, and 0.89 for System 2. Patient-based sensitivity, specificity, and AUC were 0.93, 0.73, and 0.83 for System 1, and 0.95, 0.70, and 0.83 for System 2. Although a relatively large number of false positives were observed in CAC-based assessments, side-based and patient-based performances showed improvement.

Conclusion: Side-based and patient-based performances were sufficient when calculated on the basis of CAC-based evaluations for diagnosing CACs on panoramic radiographs. When conducting studies of this type, performance assessments should include side-based and patient-based evaluations in addition to CAC-based analyses. ***(Imaging Sci Dent 20250232)***

KEY WORDS: Radiography, Panoramic; Deep Learning; Vascular Calcification

Introduction

Carotid artery calcifications (CACs), which can be reliably assessed using computed tomography (CT) and ultrasonography (US), have been reported to be associated with a range of cerebrovascular and cardiovascular events, including cerebral stroke, infarction, and coronary heart disease.[1-3] In this context, numerous studies have highlighted the potential utility of panoramic radiography as a screening tool for CACs.[4-11] However, inconsistencies persist regarding differences in disease severity between patients with unilateral and bilateral CACs detected on panoramic radiographs.[9-11] Furthermore, several CAC characteristics, including size, shape, and location, may also be associated with disease severity.[12-16] These associations may vary depending on the specific disease outcome under investigation.

While oral radiologists with specialized training in interpreting panoramic radiographs demonstrate high performance in CAC detection, achieving sensitivities exceeding 0.8, general dentists without such training show a mark-

†These authors contributed equally to this work as the first author.
Received August 22, 2025; Revised November 28, 2025; Accepted December 4, 2025
Published online January 30, 2026
*Correspondence to : Dr. Chiaki Kuwada
Department of Oral and Maxillofacial Radiology, Aichi Gakuin University School of Dentistry, 2-11 Suemori-dori, Chikusa-ku, Nagoya 464-8651, Japan
Tel) +81-52-759-2165, E-mail) chiaki@dpc.agu.ac.jp

edly lower sensitivity of 0.21.[17] To address this limitation, several deep learning (DL) systems have been developed and applied for CAC detection in panoramic radiographs, with reports of high diagnostic performance.[17-22] Given the aforementioned inconsistencies and the potential relationships between CAC characteristics and disease severity, the performance of DL-based CAC detection systems should be evaluated from 3 complementary perspectives: CAC-based, side-based, and patient-based assessments. However, most previous studies have addressed only 1 of these evaluation levels.[17,18,20,21]

Various methodological approaches have been used in the development of DL systems for CAC detection in panoramic radiographs, with differences observed in both target selection and DL functionality. Regarding target selection, 2 primary approaches may be considered: direct detection of individual CACs or classification of specific areas as containing CACs. For individual CAC detection, DL-based detection or segmentation functions can be employed, and performance can be evaluated on a CAC-specific basis. In area-based classification, 2 target regions are commonly examined: the entire panoramic radiograph or the limited bilateral cervical regions where CACs are most likely to occur. In a previous study, classification-based DL models demonstrated improved patient-based performance when determinations were made using side-based results derived from limited regions, compared with those based on the entire radiograph.[22] Alternatively, area classification may also be performed using outputs from individual CAC detection.[18,20] In such cases, the selection of target areas, whether the entire radiograph or limited regions, should be carefully considered, and performance should continue to be evaluated using side-based and patient-based assessments in addition to CAC-based results.

The present study aimed to develop 2 DL systems employing detection functions: one designed to detect calcifications across the entire panoramic radiograph and another designed to detect calcifications within the limited bilateral cervical areas. The diagnostic performance of these systems was subsequently compared using CAC-based, side-based, and patient-based evaluations.

Materials and Methods

The present study was approved by the Ethics Committee of the authors' affiliated university (approval No. 496) and was conducted in accordance with the principles outlined in the Declaration of Helsinki. Given the noninvasive and retrospective design of the study, which relied on anonymized panoramic radiographs, the Ethics Committee waived the requirement for informed consent. Nevertheless, participants were provided with an opportunity to opt out of study participation.

A total of 580 panoramic radiographs were included in the present study, consisting of 290 radiographs from patients with CACs and 290 radiographs from control subjects without CACs. Among the 290 patients with CACs, who were enrolled between 2008 and 2023, 215 exhibited bilateral CACs, whereas 75 exhibited unilateral CACs. Control subjects were selected to match the mean age and gender distribution of the CAC patient group. For supervised learning and for use as the gold standard in the DL training and testing processes, the presence or absence of CACs was determined independently by 2 oral radiologists with 8 and 38 years of experience, respectively. In cases of disagreement, final determinations were reached by consensus following discussion. Among all subjects, CAC status was verified using CT images in 142 patients and 113 control subjects. For the remaining 325 radiographs, CAC determinations were based exclusively on panoramic radiographic findings. The validation and test datasets used in the DL training and testing processes were selected from radiographs for which corresponding CT images were available as reference standards.

Panoramic radiographs were obtained using either a Veraviewepocs system (J Morita Mfg Corp., Kyoto, Japan), operated at a tube voltage of 75 kVp, tube current of 8 mA, and an exposure time of 16.2 seconds, or an AUTO IIINTR system (Asahi Roentgen Industry, Kyoto, Japan), operated at a tube voltage of 75 kVp, tube current of 12 mA, and an exposure time of 12.0 seconds. All acquired radiographs were stored in the hospital's imaging database.

Development of DL systems

Two DL systems were developed using the You Only Look Once version 7 (YOLOv7) network[23] on Windows 10 Pro with a 24 GB GPU (NVIDIA GeForce RTX 3090 Ti; NVIDIA, Santa Clara, CA, USA) and 64 GB of memory (Fig. 1).

System 1 was designed to detect individual CACs across the entire panoramic radiograph (Fig. 1A). The dataset comprised 250 images per group (CAC patient group and control group) for training and validation, with an additional 40 images per group reserved as test data (Table 1). An oral radiologist (CK) with 8 years of experience annotated all images, thereby providing supervised training and validation data as well as the gold standard for performance evaluation. Individual CACs were delineated using rectangular

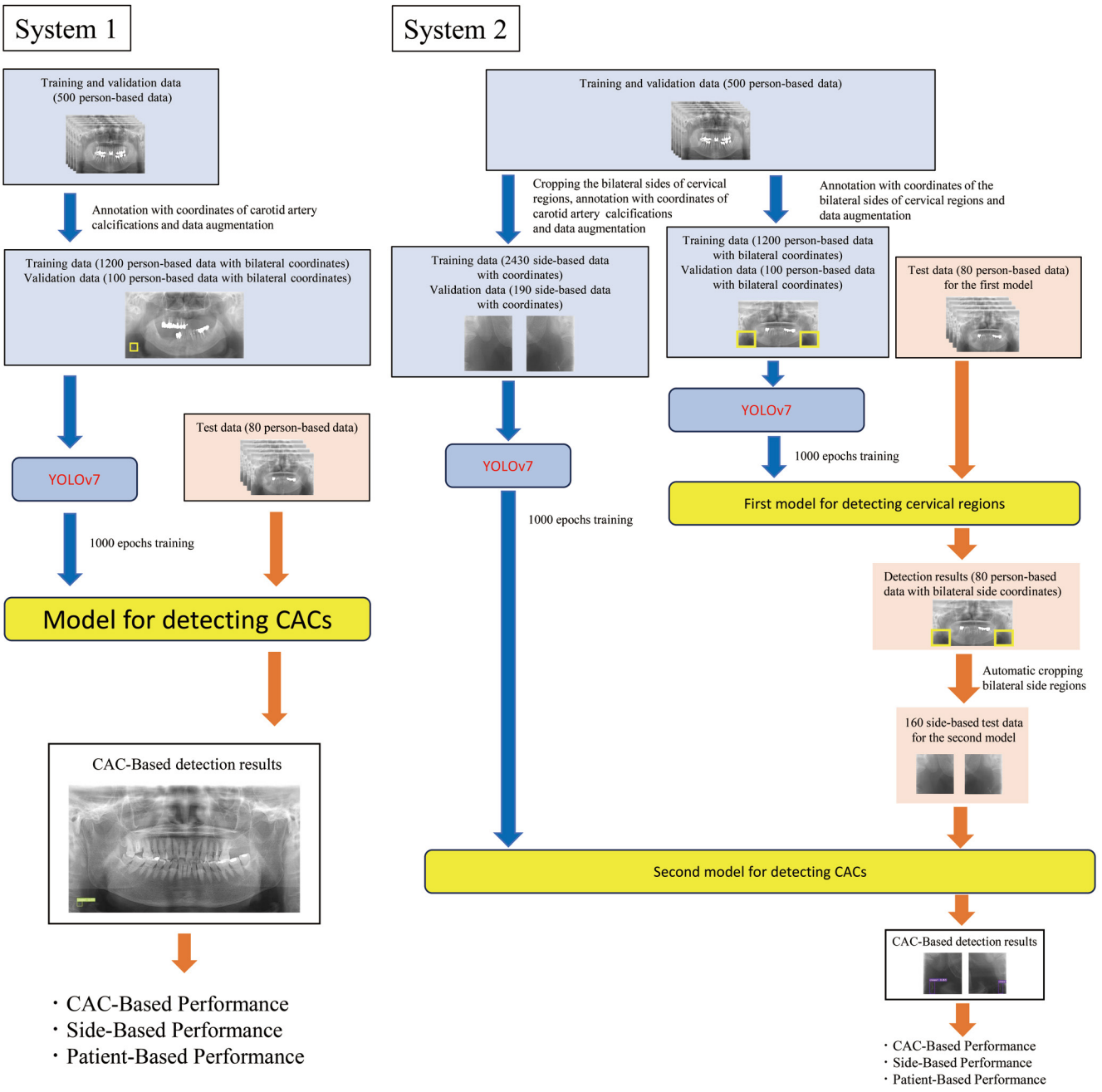

Fig. 1. Schematic representation of Systems 1 and 2. A. System 1 comprises a single detection model designed to identify individual carotid artery calcifications (CACs) across the entire panoramic radiograph. B. System 2 consists of 2 sequential detection models: the first model identifies the bilateral cervical regions in which CACs are most likely to be present, and the second model detects CACs within these regions.

bounding boxes created with the annotation tool LabelImg (https://github.com/tzutalin/labelImg), which automatically extracted coordinate information. Bounding boxes were minimized to appropriately encompass each CAC. When multiple radiopaque lesions suggestive of CACs were separated by distances greater than 3 mm, they were classified as distinct CACs. To improve model robustness, the training dataset was augmented 3 fold through brightness adjustment and horizontal flipping using Roboflow (https://roboflow.com/). Following training for 500, 600, 800, and 1,000 epochs, 4 detection models corresponding to System 1 were generated. When applied to the test dataset, the trained model automatically detected CACs and displayed bounding boxes on the panoramic radiographs (Fig. 2).

System 2 employed a 2-step detection strategy for identifying CACs within limited cervical regions (Fig. 1B). In the

Table 1. Data assignment (numbers of panoramic radiographs)

Dataset	Patient with CAC			Control without CAC
	Unilateral CAC	Bilateral CAC	Total	
Training and validation data	55	195	250	250
Test data	20	20	40	40
Total	75	215	290	290

CAC: carotid artery calcification

Fig. 2. Example of carotid artery calcification (CAC) detection using System 1. Predicted CACs are highlighted with bounding boxes across the entire panoramic radiograph.

first step, a model detected bilateral cervical regions that potentially contained CACs. A custom Python-based algorithm was subsequently applied to crop these detected regions for further analysis. Within the extracted regions, a second model was used to detect individual CACs. For the first model, cervical regions were annotated according to predefined criteria: the medial border was defined by a line parallel to the posterior edge of the image, passing through the intersection of the tongue shadow and the inferior mandibular border; the superior border was defined by a line perpendicular to the posterior edge of the image, intersecting the midpoint of the mandibular ramus height; and the posterior and inferior borders corresponded to the posterior and inferior edges of the image, respectively. For the second model, individual CACs were enclosed within bounding boxes using the same annotation protocol applied in System 1, but restricted to the cropped cervical regions. All annotations were performed by the same radiologist. CAC detection models were trained for 500, 600, 800, and 1,000 epochs. The 40 test images were initially processed by the first model to extract cervical regions, after which the cropped images were analyzed by the second model. This workflow enabled automated detection of CACs within predefined cervical regions, with bounding boxes visualized on the extracted images (Fig. 3).

Fig. 3. Example of carotid artery calcification (CAC) detection using System 2. The first model crops the bilateral cervical regions, and a secondary model subsequently detects CACs within these regions, which are visualized using bounding boxes.

Performance evaluation procedures

For CAC-based evaluation, a total of 78 rectangular regions containing CACs were analyzed. The intersection over union (IoU) was calculated based on the degree of overlap between the predicted bounding boxes and the corresponding ground truth bounding boxes. When the IoU exceeded 0.5, the detection was classified as a CAC-based true positive (cTP); otherwise, it was classified as a CAC-based false negative (cFN). When a bounding box was placed over a region that did not contain an actual CAC, the detection was recorded as a CAC-based false positive (cFP).

Performance metrics for CAC-based evaluation included recall (sensitivity, cTP/(cTP + cFN)), precision (positive predictive value [PPV], cTP/(cTP + cFP)), and the F1-score, defined as the harmonic mean of recall and precision.

Side-based evaluation was derived from CAC-based detection results. When at least 1 bounding box was detected within a cervical region that contained at least 1 true CAC, the outcome was classified as a side-based true positive (sTP). When a bounding box appeared in a cervical region that did not contain any CACs, it was labeled as a side-based false positive (sFP). When no bounding boxes were detected in a cervical region where CACs were present, the result was classified as a side-based false negative (sFN). When no bounding boxes were identified in a cervical region without CACs, the outcome was classified as a side-based true negative (sTN).

Performance metrics for side-based evaluation included sensitivity (recall, sTP/(sTP + sFN)), specificity (sTN/(sTN + sFP)), PPV (precision, sTP/(sTP + sFP)), negative predictive value (NPV, sTN/(sTN + sFN)), accuracy ((sTP + sTN)/(sTP + sFP + sFN + sTN)), and the area under the receiver operating characteristic curve (AUC).

For System 1, patient-based performance was determined directly from CAC-based detection results obtained from the entire panoramic radiograph. When at least 1 bounding box was detected in a radiograph from a patient with confirmed CACs, the case was designated as a patient-based true positive (pTP). When a bounding box appeared in a radiograph from a patient without CACs, the outcome was classified as a patient-based false positive (pFP). When no bounding boxes were detected in a radiograph containing CACs, the case was classified as a patient-based false negative (pFN). When no bounding boxes were detected in a radiograph without CACs, the outcome was recorded as a patient-based true negative (pTN).

For System 2, patient-based evaluation was derived from side-based results (Fig. 4). When at least 1 side was classified as sTP or sFP in a patient with unilateral or bilateral CACs, the case was designated as pTP. When at least 1 side was classified as sFP in a patient without CACs on either side, the case was labeled as pFP. A patient classified as sFN

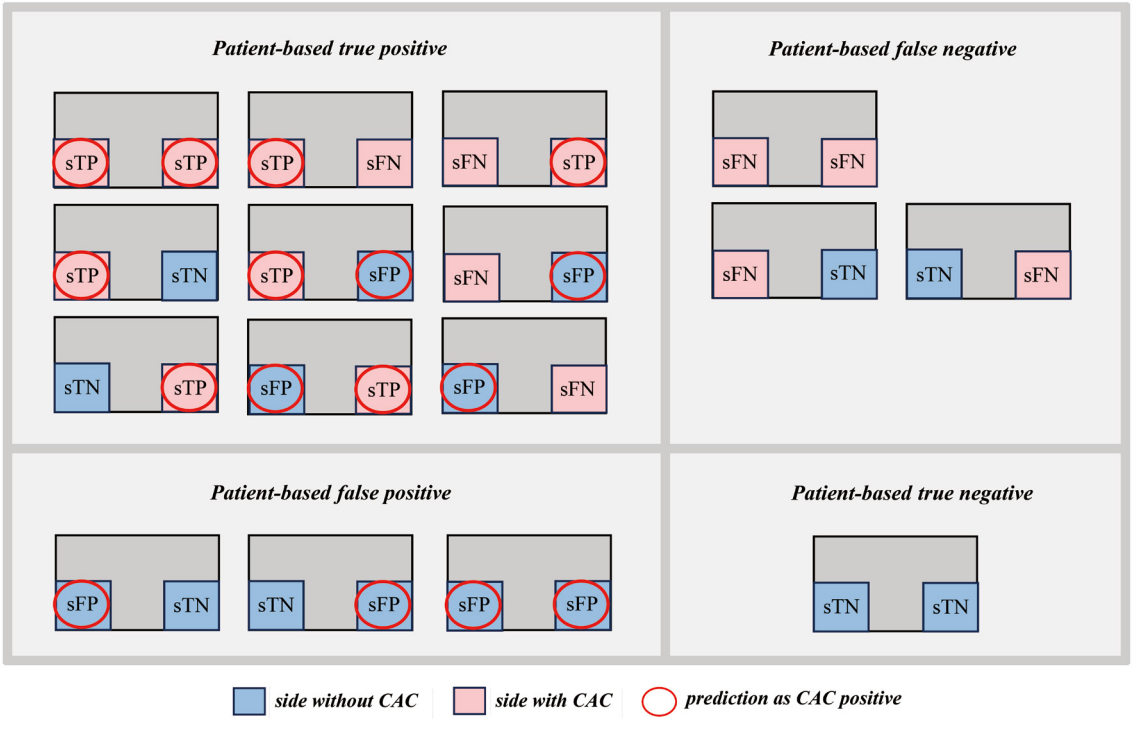

Fig. 4. Patient-based evaluations derived from side-based assessments.

on both sides, or as sFN on 1 side and sTN on the other, was designated as pFN. When both sides were classified as sTN, the case was classified as pTN.

Performance metrics for patient-based evaluation included sensitivity (recall, pTP/(pTP + pFN)), specificity (pTN/(pTN + pFP)), PPV (precision, pTP/(pTP + pFP)), NPV (pTN/(pTN + pFN)), accuracy ((pTP + pTN)/(pTP + pFP + pFN + pTN)), and AUC.

Statistical analyses

The sensitivities of CAC detection between the 2 systems were compared using the chi-square test. In addition, differences in side-based and patient-based AUCs between the 2 systems were evaluated using the DeLong test. Statistical significance was defined as a *P*-value less than 0.05.

Results

For the CAC-based analysis, all bounding boxes predicted by both systems were located within the bilateral cervical regions, which represent the most common anatomical sites for CAC occurrence. The highest F1-score for both systems was achieved by the models trained with 1,000 epochs (Table 2). Accordingly, subsequent performance evaluations were conducted using the results from these models. Out of a total of 78 CACs, Systems 1 and 2 successfully detected 63 and 70 CACs, respectively, corresponding to recall (sensitivity) values of 0.81 and 0.90. The chi-square test revealed no statistically significant difference in CAC-based sensitivity between the 2 systems. However, the relatively high number of false positives (FPs) adversely affected precision and F1-scores for both systems. Representative examples of detection results obtained from both systems are shown in Figures 5 and 6.

For the side-based analysis, the first model of System 2, which was designed to detect rectangular cervical regions potentially containing CACs, successfully identified all cervical regions (Table 3). As a result, side-based performance could be directly compared between Systems 1 and 2. The area under the receiver operating characteristic curve (AUC) values for side-based performance did not differ significantly between the 2 systems, as demonstrated by the DeLong test.

For the patient-based analysis, both systems demonstrated high sensitivity, with values exceeding 0.90 (Table 4). A chi-

Table 2. Carotid artery calcification-based performance

	Epochs	Recall (sensitivity)	Precision (PPV)	F1-score
System 1	500	0.47 (37/78)	0.80 (37/46)	0.59
	600	0.65 (51/78)	0.73 (51/70)	0.69
	800	0.68 (53/78)	0.68 (53/78)	0.68
	1000	0.81 (63/78)	0.68 (63/93)	0.74
System 2	500	0.91 (71/78)	0.62 (71/114)	0.74
	600	0.86 (67/78)	0.68 (67/99)	0.76
	800	0.90 (70/78)	0.58 (70/121)	0.71
	1000	0.90 (70/78)	0.67 (70/105)	0.77

Numbers in parentheses denote bounding boxes. PPV: positive predictive value

Table 3. Side-based performance

System	Sensitivity (recall)	Specificity	PPV (precision)	NPV	Accuracy	AUC
System 1	0.87 (52/60)	0.80 (80/100)	0.72 (52/72)	0.91 (80/88)	0.83 (132/160)	0.83*
System 2	0.93 (56/60)	0.84 (84/100)	0.78 (56/72)	0.95 (84/88)	0.88 (140/160)	0.89*

Numbers in parentheses denote sides. PPV: positive predictive value, NPV: negative predictive value, AUC: area under the receiver operating characteristic curve, *: no difference by DeLong test

Table 4. Patient-based performance

System	Sensitivity (recall)			Specificity	PPV (precision)	NPV	Accuracy	AUC
	Unilateral	Bilateral	Total					
System 1	0.95 (19/20)	0.90 (18/20)	0.93 (37/40)	0.73 (29/40)	0.77 (37/48)	0.91 (29/32)	0.83 (66/80)	0.83*
System 2	0.90 (18/20)	1.00 (20/20)	0.95 (38/40)	0.70 (28/40)	0.76 (38/50)	0.93 (28/30)	0.83 (66/80)	0.81*

Numbers in parentheses denote patients. PPV: positive predictive value, NPV: negative predictive value, AUC: area under the receiver operating characteristic curve, *: no difference by DeLong test

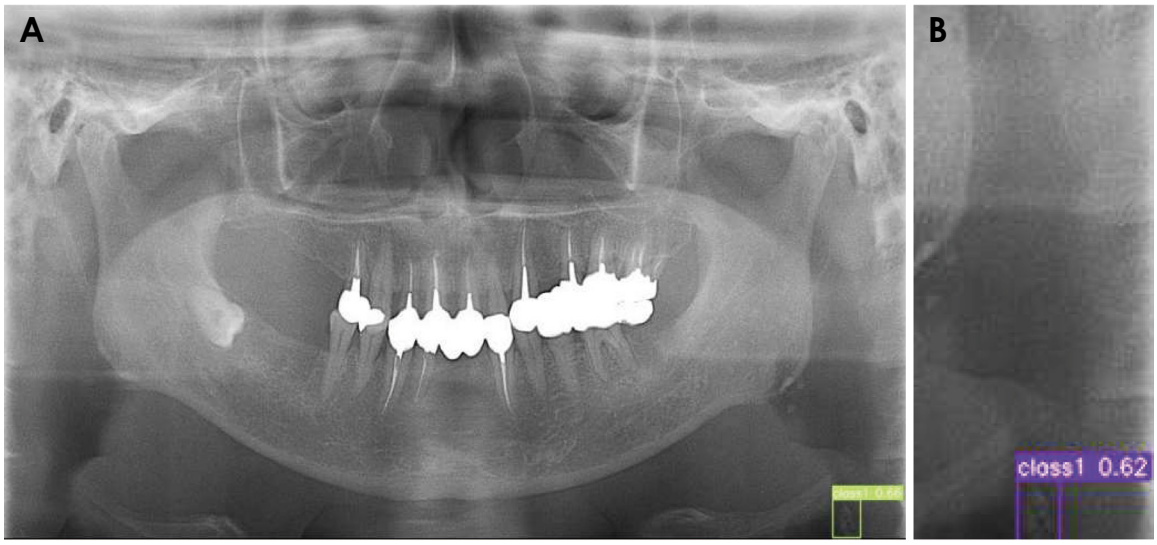

Fig. 5. A representative case with a carotid artery calcification (CAC) on the left side. Both System 1 (A) and System 2 (B) correctly detected the CAC located inferior to the hyoid bone.

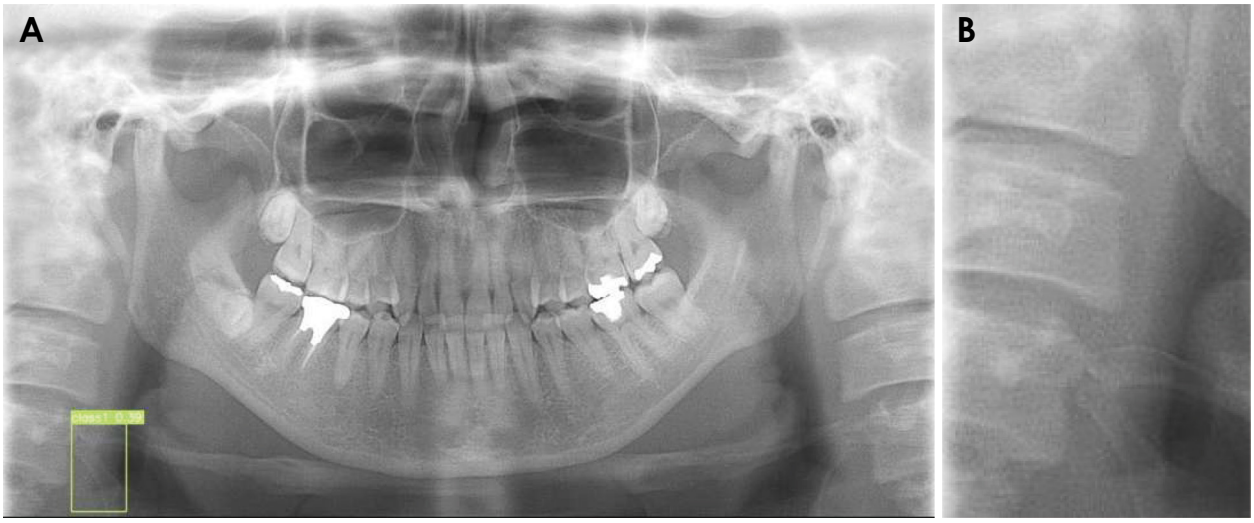

Fig. 6. A representative case with no calcifications on either side. A. System 1 detected a region in the right cervical area corresponding to a calcified thyrohyoid ligament, which connects the greater horn of the hyoid bone to the superior horn of the thyroid cartilage, as well as part of the hyoid bone. B. In contrast, System 2 did not produce any false-positive detections in the right cervical area.

square test showed no significant difference in patient-based sensitivity between patients with unilateral CACs and those with bilateral CACs for either system. The AUC values for both systems showed no statistically significant difference, as confirmed by the DeLong test.

Discussion

A key novelty of the present study is the evaluation of CACs across multiple hierarchical levels. This hierarchical assessment enables not only the identification of individual CACs, but also the estimation of their clinical relevance through side-based and patient-based evaluations, which more closely reflect the overall severity of related lesions. These findings may support earlier identification of patients at increased risk, thereby facilitating clinical decision-making. Furthermore, they may enable the integration of AI-assisted CAC detection into routine dental and medical workflows.

Although previous studies have examined CAC diagnosis using DL systems applied to panoramic radiographs, performance evaluation approaches have differed substantially de-

pending on the DL functions employed and the target regions analyzed. In many studies, evaluation criteria have not been explicitly defined. When CAC morphology and anatomical location must be assessed, the CACs themselves constitute the primary detection targets. In such contexts, DL-based segmentation or detection approaches may be particularly appropriate. In the present study, both System 1 and System 2, which relied on DL detection techniques, demonstrated relatively high recall (sensitivity) values of 0.81 and 0.90, respectively. However, precision (PPV) values were comparatively low at 0.68 and 0.67, indicating that 30 and 35 bounding boxes, respectively, were incorrectly classified as false positives (FPs). These misclassified regions included calcified anatomical structures that can resemble CACs, such as portions of the hyoid bone, cervical vertebrae, and the thyrohyoid ligament. Improving performance therefore requires reducing FPs, which may be facilitated by training with image datasets in which CACs are more rigorously verified. Although no prior studies have reported CAC-based performance metrics using methods identical to those applied here, Yoo et al.[21] evaluated CAC detection using DL-based segmentation across 5 networks, delineating and highlighting CAC regions. They reported mean Jaccard index (IoU) values slightly above 0.5, suggesting that segmented areas often included substantial non-CAC regions. While such performance may be sufficient for CAC detection, more advanced techniques may be necessary for accurate assessment of CAC shape and precise anatomical location.

Previous studies have predominantly focused on side-based evaluations using diverse methodologies and DL architectures. Katz et al.[18] employed an approach similar to that used in the present study by identifying CACs within limited regions encompassing both cervical areas, which were cropped from entire panoramic radiographs using a strategy comparable to that implemented in System 2. Using a Faster R-CNN network, they reported side-based sensitivity, specificity, and accuracy values of 0.75, 0.80, and 0.83, respectively. The side-based performance of System 2 in the present study was consistent with these findings and demonstrated slightly higher performance metrics. The comparable side-based results observed between the 2 systems in the present study suggest that, when DL detection functions are applied, either full panoramic radiographs or regionally cropped cervical images may be used effectively. In a related investigation, Yoo et al.[21] applied a DL classification function prior to segmentation. They horizontally flipped cropped right-sided cervical regions to match left-sided anatomy and classified the images according to the presence or absence of CACs, achieving high AUC values exceeding 0.95 in 4 of the 5 networks evaluated. Considering the true prevalence of CACs, Amitay et al.[19] developed DL-based classification models using 4 networks and applied them to bilateral cervical regions cropped from panoramic radiographs. Their models achieved high specificity values exceeding 0.95 but relatively lower sensitivity values of approximately 0.80, partly attributable to the large proportion of regions without CACs. Similarly, Kuwada et al.[22] applied DL-based classification to limited cervical regions and reported sensitivity values of 0.88 and 0.87. Although CAC prevalence differed across studies, side-based diagnostic performance was generally found to be adequate.

In the present study, patient-based performance for System 1 was determined on the basis of CAC-based evaluations. Recently, Vinayahalingam et al. employed Faster R-CNN and Swin Transformer architectures and reported patient-based sensitivity and specificity values of 0.881 and 0.897, respectively, using an evaluation approach similar to that applied in System 1.[20] Their reported sensitivity was lower than that observed for System 1 (0.93), whereas their specificity was higher. Patient-based performance for System 2, which was derived from side-based evaluations, demonstrated a high sensitivity of 0.95 but a relatively low specificity of 0.70, with an AUC of 0.83, showing no statistically significant difference compared with System 1. From the perspective of developing a fully automated system, System 1 may be advantageous because it eliminates the need for bilateral cervical region cropping. Although a DL classification function rather than a DL detection function was used for cervical region classification, Kuwada et al.[22] similarly derived patient-based performance from side-based assessments, following an approach comparable to that used in the present study. They reported an AUC of 0.90, which was higher than that achieved by System 2 (0.83). However, additional validation using larger datasets is required to determine whether DL detection or DL classification approaches are more appropriate for this type of evaluation. Based on side-based sensitivity and specificity values, Amitay et al. proposed formulas for estimating patient-based performance.[19] When these formulas were applied to the results of System 2, the estimated patient-based sensitivity, specificity, and accuracy values were 0.94, 0.74, and 0.81, respectively, which were approximately consistent with the actual observed values (Table 4). Although further validation is necessary, this estimation approach may serve as a useful tool for approximating patient-based performance.

This study has several limitations. First, the dataset was obtained from a single institution, and its relatively small

size limits the generalizability of the findings. To address this limitation, larger datasets should be collected from multiple institutions, and external validation studies should be conducted. Second, the presence or absence of CACs was not verified using CT for all panoramic radiographs. Although the validation and test datasets were selected from cases with CT verification, thereby ensuring reliable evaluation results, comprehensive CT confirmation for all images would further strengthen model performance and reliability. Third, with respect to the number of epochs used for CAC detection model training, 1,000 epochs produced the best performance among the conditions examined in the present study; however, it remains unclear whether further increases in the number of training epochs would yield additional performance gains. This issue should be explored in future investigations. Fourth, the present study did not account for CAC shape or anatomical location. Because these characteristics are important for estimating disease severity, future studies should examine them in greater detail, potentially through the application of DL-based segmentation methods to enable more precise analyses.

In conclusion, side-based and patient-based performance metrics were found to be sufficient when derived from individual CAC-based evaluations for the diagnosis of CACs on panoramic radiographs. When conducting studies on CAC diagnosis using panoramic radiographs, performance assessments should incorporate side-based and patient-based evaluations in addition to CAC-based analyses.

Conflicts of Interest: None

References

1. Wintermark M, Jawadi SS, Rapp JH, Tihan T, Tong E, Glidden DV, et al. High-resolution CT imaging of carotid artery atherosclerotic plaques. AJNR Am J Neuroradiol 2008; 29: 875-82.
2. Gaitini D, Soudack M. Diagnosing carotid stenosis by Doppler sonography: state of the art. J Ultrasound Med 2005; 24: 1127-36.
3. Cohen GI, Aboufakher R, Bess R, Frank J, Othman M, Doan D, et al. Relationship between carotid disease on ultrasound and coronary disease on CT angiography. JACC Cardiovasc Imaging 2013; 6; 1160-7.
4. Ohba T, Takata Y, Ansai T, Morimoto Y, Tanaka T, Kito S, et al. Evaluation of calcified carotid artery atheromas detected by panoramic radiograph among 80-year-olds. Oral Surg Oral Med Oral Pathol Oral Radiol Endod 2003; 96: 647-50.
5. Alves N, Deana NF, Garay I. Detection of common carotid artery calcifications on panoramic radiographs: prevalence and reliability. Int J Clin Exp Med 2014; 7: 1931-9.
6. Prados-Privado M, García Villalón J, Blázquez Torres A, Martínez-Martínez CH, Prados-Frutos JC, Ivorra C. Are panoramic images a good tool to detect calcified carotid atheroma? A systematic review. Biology (Basel) 2022; 11: 1684.
7. de Oliveira GA, de Sá CR, Junior OR, Santos RP, Manzi FR. Case reports of a new method for differential diagnosis of calcified carotid artery atheroma. Case Rep Dent 2021; 2024: 8874087.
8. Smoljan-Basuga M, Marelić M, Badel T, Škrinjar I, Lončar-Brzak B, Klemenčić A, et al. Significance of calcifications in projection of carotid arteries on orthopantomography for detection of carotid artery stenosis. Acta Stomatol Croat 2022; 56: 257-66.
9. Gustafsson N, Ahlqvist JB, Näslund U, Wester P, Buhlin K, Gustafsson A, et al. Calcified carotid artery atheromas in panoramic radiographs are associated with a first myocardial infarction: a case-control study. Oral Surg Oral Med Oral Pathol Oral Radiol 2018; 125: 199-204.
10. Garoff M, Ahlqvist J, Edin LT, Jensen S, Levring Jäghagen E, Petäjäniemi F, et al. Bilateral vessel-outlining carotid artery calcifications in panoramic radiographs: an independent risk marker for vascular events. BMC Cardiovasc Disord 2019; 19: 225.
11. Gustafsson N, Ahlqvist J, Norhammar A, Näslund U, Rydén L, Wester P, et al. Association of high cardiovascular risk and diabetes with calcified carotid artery atheromas depicted on panoramic radiographs. Oral Surg Oral Med Oral Pathol Oral Radiol 2022; 133: 88-99.
12. Nandalur KR, Baskurt E, Hagspiel KD, Finch M, Phillips CD, Bollampally SR, et al. Carotid artery calcification on CT may independently predict stroke risk. AJR Am J Roentgenol 2006; 186: 547-52.
13. Alman AC, Johnson LR, Calverley DC, Grunwald GK, Lezotte DC, Hokanson JE. Validation of a method for quantifying carotid artery calcification from panoramic radiographs. Oral Surg Oral Med Oral Pathol Oral Radiol 2013; 116: 518-24.
14. Wannarong T, Parraga G, Buchanan D, Fensre A, House AA, Hackam DG, et al. Progression of carotid volume predicts cardiovascular events. Stroke 2013; 44: 1859-65.
15. Lu M, Cui Y, Peng P, Qiao H, Cai J, Zhao X. Shape and location of carotid atherosclerotic plaque and intraplaque hemorrhage: a high-resolution magnetic resonance imaging study. J Atheroscler Thromb 2019; 26: 720-7.
16. Bladh M, Gustafsson N, Engström G, Kennbäck C, Klinge B, Nilsson PM, et al. Defined shapes of carotid artery calcifications on panoramic radiographs correlate with specific signs of cardiovascular disease on ultrasound examination. Oral Durg Oral Med Oral Pathol Oral Radiol 2024; 137: 408-20.
17. Song YB, Jeong HG, Kim C, Kim D, Kim J, Kim HJ, et al. Comparison of detection performance of soft tissue calcifications using artificial intelligence in panoramic radiography. Sci Rep 2022; 12: 19115.
18. Kats L, Vered M, Zlotogorski-Hurvitz A, Harpaz I. Atherosclerotic carotid plaque on panoramic radiographs: neural network detection. Int J Comput Dent 2019; 22: 163-9.
19. Amitay M, Barnett-Itzhaki Z, Sudri S, Drori C, Wase T, Abu-El-Naaj I, et al. Deep convolution neural network for screening carotid calcification in dental panoramic radiographs. PLOS Digit Health 2023; 2: e0000081.
20. Vinayahalingam S, van Nistelrooij N, Xi T, Heiland M, Bressem K, Rendenbach C, et al. Detection of carotid plaques on pan-

oramic radiographs using deep learning. J Dent 2024; 151: 105432.
21. Yoo SW, Yang S, Kim JE, Huh KH, Lee SS, Heo MS, et al. CACSNet for automatic robust classification and segmentation of carotid artery calcification on panoramic radiographs using a cascaded deep learning network. Sci Rep 2024; 14: 13894.
22. Kuwada C, Mitsuya Y, Fukuda M, Yang S, Lise Y, Mori M, et al. Area detection improves the person-based performance of a deep learning system for classifying presence of carotid artery calcification on panoramic radiographs. Oral Radiol 2026; 42: 91-100.
23. Wang CY, Bochkovskiy A, Liao HY. YOLOv7: trainable bag-of-freebies sets new state-of-the-art for real-time object detectors. In: Proceedings of the IEEE/CVF Conference on Computer Vision and Pattern Recognition (CVPR); 2023 Jun; Vancouver, Canada. IEEE; 2023. p. 7464-75.